Article

# Investigation of Correlation Between Self-Calibration Parameters of Terrestrial Laser Scanner (TLS)

**Mansoor Sabzali*[1] and Lloyd Pilgrim[2]**

[1]PhD Student, [2]Senior Lecturer, Civil, Surveying and Environmental Engineering Discipline, Newcastle University

University Dr, Callaghan NSW 2308, Australia

Email: mansoor.sabzali@uon.edu.au

Email: lloyd.pilgrim@newcastle.edu.au

Received: November 14, 2023; Accepted: December 27, 2023; Published: January 17, 2024

## ABSTRACT

To determine the robust self-calibration approach for Terrestrial Laser Scanner (TLS), the profound knowledge of Geodetic Network Design and Photogrammetry is required. For any photogrammetric tasks, three main predefined criteria - precision, correlation, and uncertainty of parameters - play more vital roles than other criteria. Geodetic network design is composed of four interrelated design orders: zero, first, second and third order of design to fulfil the mentioned criteria. Zero order design which is the core focus of this research reveals the correlation between estimated parameters in self-calibration of TLS. In other words, three types of the parameters - calibration parameters (CP), exterior orientation parameters (EOP), and object points (OP) – as unknowns must be solved through bundle block adjustment (BBA) of TLS self-calibration. The current parametrization of exterior orientation used for TLS calibration, unlike camera calibration, is limited to collinearity conditions from one scan station. According to established concepts in computer vision, by adding the constraints of relative orientation (RO) to bundle block adjustment, the estimations of unknowns will be in higher quality and potentially lower correlation. Therefore, the application of this principle must determine more precise and lower correlated parameters for TLS self-calibration. This research will evaluate the correlation of TLS self-calibration parameters between collinearity and proposed coplanarity conditions and will identify the potential improvements in correlation and precision of the parameters with the aid of the new formulation. An experiment of self-calibration was undertaken using Leica ScanStation P50 and implemented on MATLAB codes.

**KEY WORDS:** collinearity, coplanarity, correlation, precision, self-calibration

## 1. INTRODUCTION

Laser scanner is an active electro-optical sensor using the laser as the main source of illumination to capture the spatial data through the availability of the reflected signal from a scene. With the advent of first generation of laser scanners, data acquisition approaches in Photogrammetry and Engineering Geodesy have been revolutionised. Currently, the position of laser scanners especially with the terrestrial platform for data collection – terrestrial laser scanners (TLS) – is increasingly dominating in the other disciplines, particularly deformation monitoring, in order to guarantee the highly accurate deliverables.

Thus, the application of TLS based on the technical specifications provided by manufacturers can be acceptable within or under certain conditions of scanning configuration. On the other hand, the limitation imposed by manufacturers for providing the confidential information about manufacturer-oriented calibration procedure in the design and calibrating TLS and the consideration of a subset of unknown systematic errors are the second and third highlighted motivation of TLS calibration. Fourthly, the determination of the internal characteristics of every sensor provides a metric tool in Photogrammetry and Engineering Geodesy for data acquisition, similar to investigation of the interior orientation parameters of a camera.

In this research, the sophisticated self-calibration principle of TLS from the perspective of geodetic network design with the major emphasise on zero order design (ZOD) will be aimed. It results in a new parametrization of exterior orientation parameters (EOP) of self-calibration to control the existing correlation between estimated parameters.

## 2. LITERATURE REVIEW

The literature review contains the brief introductory of TLS, identification of the error sources of 3D point cloud measurements, and photogrammetric methods alongside geodetic network design concepts for the creation of self-calibration of TLS.

### 2.1 Terrestrial laser scanner (TLS)

TLS is a terrestrial laser-based instrument which delivers the 3D point coordinates in 3D spherical coordinates. In principle, TLS is a very high-speed and movable total station which is able to capture millions of points in a second as the consequence of measuring three spherical coordinates, range $r$, horizontal angle $h$ and vertical angle $v$ from the returned signal reflected from a single point received at TLS.

The conversion from 3D spherical into Cartesian coordinates is represented as follows:

$$\begin{bmatrix} x_i \\ y_i \\ z_i \end{bmatrix}_{i=1\dots n} = \begin{bmatrix} r_i \cos v_i \cos h_i \\ r_i \cos v_i \sin h_i \\ r_i \sin v_i \end{bmatrix}_{i=1\dots n} \tag{1}$$

The index $i$ indicates the number of measured points from $1$ to $n$.

Reversely, the transformation can be applied from 3D Cartesian to spherical coordinates:

$$\begin{bmatrix} r_i \\ v_i \\ h_i \end{bmatrix}_{i=1\dots n} = \begin{bmatrix} \sqrt{x_i^2 + y_i^2 + z_i^2} \\ \tan^{-1}(\frac{z_i}{\sqrt{x_i^2 + y_i^2}}) \\ \tan^{-1}(\frac{y_i}{x_i}) \end{bmatrix}_{i=1\dots n} \tag{2}$$

Similar to any geodetic measurements, the observations are prone to be contaminated as the results of deviations called errors. The systematic errors for TLS which can be mathematically modelled namely are instrumental imperfections, atmospheric effects, scanning geometry and measurement configuration, and object and surface related issues. Although all impacts simultaneously affect the entire configuration of scanning, the separation here is made to detach the scanner with scanning self-calibration. The underlying assumption here is the self-calibration of the scanner is only influenced as the result of instrumental imperfections, meaning that the influences of the remaining errors on TLS observations are considerably minor.

Therefore, the corrected range and angular measurements $[r_c \quad h_c \quad v_c]$ as a function of observed values $[r_o \quad h_o \quad v_o]$ and corresponding correction factors of instrumental imperfections $[dr_{i.i} \quad dh_{i.i} \quad dv_{i.i}]$ are represented as below:

$$\begin{aligned} r_c &= f(r_o,\ v_o, h_o, dr_{i.i}) \\ v_c &= f(r_o,\ v_o, h_o, dv_{i.i}) \\ h_c &= f(r_o,\ v_o, h_o, dh_{i.i}) \end{aligned} \tag{3}$$

## 2.2 Instrumental imperfections (i.i)

The instrumental misalignments and irregularities in the design and production of scanners are referred to as i.i in this paper. Here, only five additional parameters (calibration parameters (CP)) relating to physical systematic errors of i.i (i.e., $a_1$ is the constant zero offset, $a_2$ is transit offset, $a_3$ is vertical angle index offset, and $a_4$ and $a_5$ are mirror offset and mirror tilt angle, respectively) which are randomly selected for this investigation, and three empirical parameters as those being formulated based on several experiments and the analysis of the residuals ($ER, EV$ and $EH$) are considered. The formulation of those calibration parameters with respect to the measurements will be given as follows:

$$dr_{i.i} = a_1 + a_2 \sin(v_o) + ER$$
$$dv_{i.i} = \frac{a_2 \cos(v_o)}{r_o} + a_3 + EV \quad (4)$$
$$dh_{i.i} = \frac{a_4}{r_o \sin(v_o)} + \frac{2a_5}{\sin(v_o)} + EH$$

It is worth mentioning the current parametrization of i.i was reported by (Muralikrishnan , et al., 2015), and there are many more calibration parameters involved, but not considered in this research.

There are several ways proposed to calibrate the TLS, similar to procedures taken for camera calibration. In brief, the component calibration concentrates on the calibrating of each component of misalignment individually using dedicated equipment and procedures resulting in separate result for corresponding components (Holst , et al., 2014; Lichti , 2007; Muralikrishnan , 2021). The examples of the component calibrations include calibration with the aid of pre-calibrated artifacts, in situ calibration, or a calibrated network of targets in volume measurements (Reshetyuk, 2009; Reshetyuk, 2010; Jafar , et al., 2018). On the other hand, the system calibration is carried out through the system using the knowledge of components and their interactions. This is completed, in a majority of applications, through self-calibration (Holst , et al., 2018; Pareja , et al., 2013; Kresten & Lindstaedt , 2022; Li, et al., 2018; Li, et al., 2018; Medic, et al., 2019). The system self-calibration requires the knowledge of photogrammetry, and it incorporates the study of geodetic network design (Lichti, et al., 2021). Since not only are the calibration parameters (Equation 4) estimated through self-calibration, but there are also two other types of unknowns including exterior orientation parameters (EOP) of every scan station and object points (OP) must be estimated through the establishment of bundle block adjustment (BBA).

### 2.3 Photogrammetric perspective

In photogrammetry, the structure from motion (SFM) process solves the exterior orientation parameters (EOP) via several BBA techniques. Considering the problem of TLS self-calibration, BBA that solve the EOP via collinearity conditions has been widely studied. The current representation of BBA of self-calibrated TLS network will be as follows:

$$x_i^j = R_{11}(X_i - X_S) + R_{21}(Y_i - Y_S) + R_{31}(Z_i - Z_S)$$
$$y_i^j = R_{21}(X_i - X_S) + R_{22}(Y_i - Y_S) + R_{23}(Z_i - Z_S) \quad (5)$$
$$z_i^j = R_{31}(X_i - X_S) + R_{32}(Y_i - Y_S) + R_{33}(Z_i - Z_S)$$

where $[x_i^j \quad y_i^j \quad z_i^j]$ = 3D point coordinates of a point $i$ in the scanner $j$ coordinate system,
$[X_i \quad Y_i \quad Z_i]$ = the corresponding object space coordinate of point $i$,
$[X_S \quad Y_S \quad Z_S]$ = scanner position $S$ in the object coordinate system, and
$R$ = element of rotation matrix including three Euler rotation angles $\omega, \phi$ and $\kappa$ around three axes.

Given equations 2, 4 and 5, BBA via collinearity equations attempt to estimate three types of unknowns: exterior orientation parameters (EOP) for each scan station ($j$) (three translations ($X_S, Y_S$ and $Z_S$), and three orientations ($\omega, \phi$ and $\kappa$)), eight calibration parameters (CP), and 3D object point coordinates (object points (OP) ($X_i, Y_i$ and $Z_i$)). The number of unknowns will be given $m = 6(j) + 8 + 3n$, while the number of measurements for the entire block will be $n = 3\ (j)\ n$. Considering the definition of the datum and the existence of at least two scan stations, a minimum of eight known observations must be given to solve those parameters.

## 2.4 Correlation and precision

Two of the most important criteria of BBA of a self-calibration network are correlation and precision of estimated parameters. The ideal situation will be guaranteed by having lower correlation and higher precision for the parameters. In principle, the precision of the parameters is judged as the results of the inversion of the Normal Matrix $N$, leading to variance and covariance matrix of unknowns in least square adjustment, and the dependency between variables called correlation is justified as the result of the computation of Pearson's coefficient which is the ratio between covariances $\sigma_{x_1x_2}$ and variances of two variables $\sigma_{x_1}$ and $\sigma_{x_2}$.

$$\rho_{x_1x_2} = \frac{\sigma_{x_1x_2}}{\sigma_{x_1}\sigma_{x_2}} \quad (6)$$

The closer to zero, the lower correlations, whereas highly correlated parameters are identified as close to $-1$ or $+1$. (Gruen. A., 2010) acknowledged, in camera calibration, correlation parameters higher than 0.9 will not be acceptable for photogrammetric tasks. In this research, the higher correlation than 0.7 is regarded as the potentially correlated parameters, and higher than 0.9 corresponds to highly correlated parameters.

Four correlation analysis between estimated parameters (CP and EOP, CP and OP, and OP and EOP) and inter-parameters must be considered. However, only the most important one which is between CP and EOP ($\rho_{cp,eop}$) will be investigated here.

## 2.5 Geodetic network design

Geodetic network design composes of four interrelated orders to design the optimal geodetic network for the surveying tasks. The fundamental idea of geodetic network optimization is to recognize whether it is possible to determine the desirable quality of network before any observations are made (Grafarend, 1974; Amiri-Simkooei, 1998; Amiri-Simkooei, et al., 2012). The initial order of optimization of a geodetic network embraces the zero order design (ZOD) focusing on the problem of optimal datum design. The major investigation of optimal datum definition is to create the Normal matrix of least square adjustment invertible by removing its datum deficiency to make it full rank. In the 3D network, the datum will be presented via formerly defining seven datum parameters (three rotations, three translations and one scale) (i.e., at least three point coordinates must be known). The entire process of ZOD influences the correlation quality between individual estimated unknowns. To resolve the issue, minimal datum (free network, or inner constraints) has been tried for self-calibration of TLS which both approaches lead to unsuccessful results due to the rise in correlation between parameters (Lichti , 2007; Reshetyuk, 2010).

The remaining orders of network such as first order design (FOD) and second order design (SOD), must be indeed addressed for the whole geodetic network design concentrating on the other criteria (Lichti, et al., 2021). However, those will be expressed in future research.

# 3. METHODOLOGY

In the literature review, the concept of implementing of ZOD to reveal the correlation between the estimated parameters and unsuccessful results in definition of invariant quantities for the datum (free network, or inner constraints) for self-calibration of TLS was shortly stated (Lichti , 2007). Thus, to have the profound knowledge of EOP might assist in predicting the lower correlation between parameters of CP and EOP (Fraser, 2001; Mikhail , et al., 2001). It is inferred that the application of other SFM approaches, apart from solely collinearity conditions, can enhance the result of BBA.

(Fraser, 2001) demonstrated determinability of camera calibration parameters and EOP is greatly enhanced by adding the constraints of relative orientations parameters (ROP) to the BBA, and more precise camera calibration parameters might lower their correlations. In other words, rather than one-step exterior orientation, relative orientation plus absolute orientation of at least two images will be implemented in bundle block adjustment. Accordingly, the relative orientation parameters will be stepwise added to block adjustment to estimate the parameters. It would potentially increase the precision and decrease the correlation of parameters of TLS.

In analytical photogrammetry, the corresponding methodology will be fulfilled as the result of fixing the EOP of one image (here the first scan station is assumed to be zero) and to define at least one constraint of relative orientation - the *base* - for one translation of the second image (here the second scan station) (i.e., distance between two origins of scanner coordinate systems is called base). Having the constraint of relative orientation helps the reconstruction of coplanarity conditions (to enhance the precision and correlation of EOP and CP) with the existence of collinearity conditions (to derive the object point coordinates in self-calibration procedure).

Figure 1 shows the collinearity conditions and coplanarity conditions of two consecutive images. Here, the entire configuration is implemented on two scan stations.

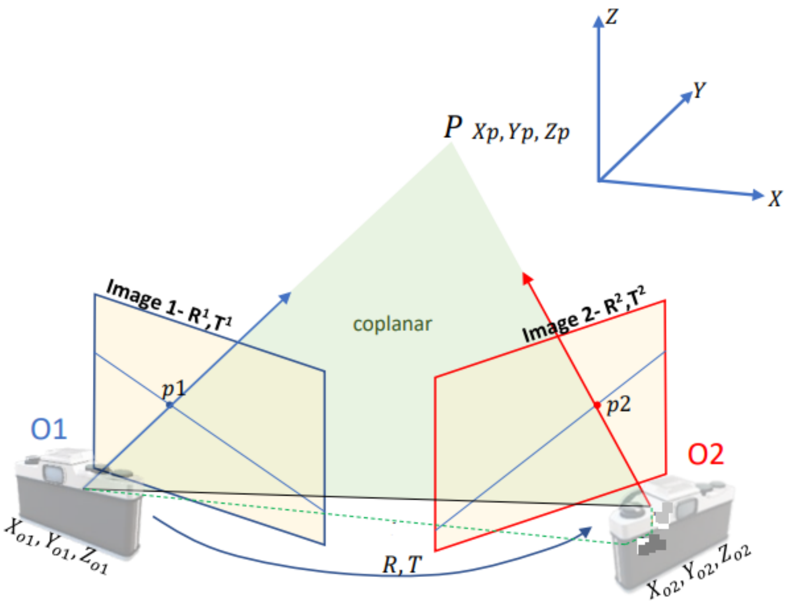


Figure 1. Collinearity and coplanarity conditions (Alsadik & Abdulateef, 2022).

Hence, when the relative orientation of two scan stations is solved, coplanarity constraints between them can be automatically constructed, and those conditions constrain the collinearity conditions. In case of more than two scan stations, the constraint of base must be again defined and added between each two stations. The configuration also allows adding more than one constraint of RO to construct the coplanarity conditions. Consequently, the availability of these constraints in collinearity equations will produce the unknowns in the reference back to the first scanner station coordinates which is assumed to be fixed.

Therefore, based on two scan stations, instead of the typical collinearity conditions of separate scan station solving 6 EOP for each scan station, we have only to estimate 5 EOP of the second scan stations (in case of the existence of one constraint), given the EOP of the first scan station as known. Additionally, so far, CP have been considered to be bundle- and block-invariant giving $m = 5 + CP + 3\,OP$; however, in case of bundle-variant CP, the number of unknows will increase to $m = 5 + 2\,CP + 3\,OP$. Due to the nature of the problem, the iterative nonlinear least square adjustment (NLSA) must be applied to determine those parameters.

It is worthwhile to note that there are numerous principles in compute vision such as Direct Linear Transformation (DLT) and the application of the projective matrix that can be alternatively applied to TLS calibration. However, those have not been studied so far. More interested readers are recommended to (El-Ashmawy, 2015).

## 4. DATA ANALYSIS AND DISCUSSION

The aim of the ZOD in geodetic network design is the definition of datum in the reasonable manner leading to lowering the existing correlation between the estimated parameters. Both conditions – collinearity conditions from one single scan station and collinearity conditions with the constraints of coplanarity conditions - have been implemented on the same data set in order to check and investigate the correlation and precision of the parameters. The field experiment through laboratory configuration at the Callaghan campus of the University of Newcastle, New South Wales, Australia was finalised on 29th May 2023 (Figure-2). Regarding the other systematic errors of TLS, particularly atmospheric effects, the lab test was undertaken with no variations of atmosphere during the measurements. The calibration test field was adjusted to be at $24\ °\mathrm{C} \pm 0.5\ °\mathrm{C}$.

Figure 2. The laboratory configuration.

Setting targets on the walls and the floor prior to data collection took approximately 4 hours of the measurement time. The data collection from two scan station was completed via the Leica ScanStation P50[1] whose range and angular accuracy are $1.2\,mm + 10\,ppm$ and 8", respectively, as reported by Leica. The post processing steps included the manual selection of 92 corresponding points of targets from two separate scan station through Leica Register 360[2] as the input for initiating the nonlinear least square adjustment to validate the approximations of eight calibration parameters of each scan station, six or five exterior orientation parameters of the second scan station, depending on the conditions, and object points. The NLSA converged after the $6^{th}$ iteration with a difference of $\pm 0.8 \times 10^{-4}\,m$ from the threshold (measured slope distance between two scan stations). All slope distances were measured by Leica Nova MS60 Total Station with range uncertainty of $1\,mm + 1.5\,ppm$ to the prism[3].

The following Tables summarise the precision of the selected parameters, resulting in the correlation investigations of the parameters.

The precision of parameters in both conditions have been carried out and

[1] https://leica-geosystems.com/products/laser-scanners/scanners/leica-scanstation-p50_new

[2] https://leica-geosystems.com/products/laser-scanners/software/leica-cyclone/leica-cyclone-register-360

[3] https://leica-geosystems.com/products/total-stations/multistation/leica-nova-ms60

highlighted in Table 1. It is understandable that the rotational angles of EOP–$\omega$ and $\varphi$- are not precisely estimated in both conditions, and notably adding the constraint in translation $Y_S$ (as the base) causes the imprecise estimation of more parameters ($\kappa, X_S, EH$ and $Y$). It means that the horizontal plane becomes totally inconsistent. The fact leads to more correlated calibration parameters in the horizontal plane (Table 2). Regarding the CP, the precision of vertical angle parameters (i.e., $a_2$ transit offset, $a_3$ vertical angle index offset and assumed empirical error of vertical angles $EV$) is not acceptable under both conditions. One of the prominent reasons for this result can be the lack of targets on the tall ceiling which due to unflattens of the roof, we were not able to set the targets (Figure 2). The second reason can be the existence of outliers in the observations. To sum up, it is concluded that adding one constraint of the base in the direction of $Y_S$ is not adequate to have the precise estimation of CP.

Table 2 illustrates the correlation matrix between EOP and CP which is the most important existing correlation. It can be seen that under the collinearity conditions, only $X_S$ and $\kappa$ can be approximated with no correlation with CP. The remaining EOP are not separatable. Interestingly, all correlations exist with only range and vertical angle CP, meaning that under the collinearity condition, decorrelated estimation of horizontal angle CP are guaranteed.

Adding the constraint in the direction of $Y_S$ results in more correlated CP with $\kappa$ and $X_S$. This is totally different from collinearity conditions. They also experience the highest correlation coefficients (close to $\pm 1$ regardless of their directions) with three calibration parameters - $ER$ empirical errors in range, $a_1$ constant zero offset in range and empirical error of horizontal angle $EH$. Additionally, the identical correlation in terms of the value and direction exists between $\omega, \varphi$ and $Z_S$ and CP under both conditions. The results were anticipated due to the lower precision outcome in Table 1.

To sum up, the constraint of $Y_S$ will not be the best choice to decrease the correlation of TLS calibration parameters, given the scanning configuration and existence of outliers. Due to this fact, Table 3 and 4 prove the precision and correlation of the parameters in case of adjusting $X_S$ as the base constraint rather than $Y_S$.

Table 1. Precision ($1\sigma$) of the selected parameters under both conditions.

| Parameters | | | Precision: Collinearity Conditions | Precision: Collinearity Conditions with one Coplanarity Constraint |
|---|---|---|---|---|
| Exterior Orientation Parameters (EOP) Second Station | | $\omega$ | 24” | 24” |
| | | $\varphi$ | 7” | 7” |
| | | $\kappa$ | 1.5” | 27” |
| | | $X_S$ | 0.08 $mm$ | 2 $mm$ |
| | | $Y_S$ | 0.4 $mm$ | – |
| | | $Z_S$ | 2 $mm$ | 1 $mm$ |
| Calibration parameters (CP) | First station | $ER$ | 0.2 $mm$ | 0.2 $mm$ |
| | | $EH$ | 1” | 55” |
| | | $EV$ | 11” | 11” |
| | | $a_1$ | 0.2 $mm$ | 0.2 $mm$ |
| | | $a_2$ | 0.6 $mm$ or $2'7''$ | 0.6 $mm$ or $2'7''$ |
| | | $a_3$ | 11” | 11” |
| | | $a_4$ | 4” | 4” |
| | | $a_5$ | 0.2” | 0.2” |
| | Second station | $ER$ | 0.2 $mm$ | 0.2 $mm$ |
| | | $EH$ | 1.5” | 28” |
| | | $EV$ | 13” | 14” |
| | | $a_1$ | 0.2 $mm$ | 0.2 $mm$ |
| | | $a_2$ | 2 $mm$ or $6'15''$ | 2 $mm$ or $6'5''$ |
| | | $a_3$ | 14” | 14” |
| | | $a_4$ | 4” | 4” |
| | | $a_5$ | 0.2” | 0.2” |
| Object Points (OP) | | $X$ | 0.3 $mm$ | 0.3 $mm$ |
| | | $Y$ | 0.1 $mm$ | 0.9 $mm$ |
| | | $Z$ | 0.2 $mm$ | 0.2 $mm$ |

Table 2. Correlation matrix between CP of both scan stations and EOP of the second scan station.

| Collinearity Conditions | | Calibration Parameters (CP): First Station | | | | | | | | Second Station | | | | | | | |
|---|---|---|---|---|---|---|---|---|---|---|---|---|---|---|---|---|---|
| | | $ER$ | $EH$ | $EV$ | $a_1$ | $a_2$ | $a_3$ | $a_4$ | $a_5$ | $ER$ | $EH$ | $EV$ | $a_1$ | $a_2$ | $a_3$ | $a_4$ | $a_5$ |
| Exterior Orientation Parameters (EOP) | $\omega$ | **0.71** | -0.10 | **-0.96** | **0.71** | **0.96** | **-0.96** | 0.07 | -0.07 | **0.73** | 0.44 | **-0.97** | **0.73** | 0.49 | **-0.97** | -0.08 | 0.08 |
| | $\varphi$ | -0.60 | 0.08 | **0.86** | -0.60 | **-0.85** | **0.86** | -0.05 | 0.05 | -0.59 | -0.37 | **0.79** | -0.59 | -0.37 | **0.79** | 0.05 | -0.06 |
| | $\kappa$ | -0.58 | 0.11 | 0.46 | -0.58 | -0.50 | 0.46 | -0.27 | 0.27 | -0.57 | 0.27 | 0.45 | -0.57 | -0.29 | 0.45 | 0.32 | -0.33 |
| | $X_S$ | -0.63 | 0.13 | 0.27 | -0.63 | -0.33 | 0.27 | -0.30 | 0.30 | -0.58 | 0.01 | 0.26 | -0.58 | -0.21 | 0.26 | 0.20 | -0.20 |
| | $Y_S$ | **-0.90** | 0.03 | 0.67 | **-0.90** | **-0.73** | 0.67 | -0.02 | 0.02 | **-0.91** | -0.52 | **0.71** | **-0.91** | -0.49 | **0.71** | 0.03 | -0.02 |
| | $Z_S$ | -0.36 | 0.01 | 0.33 | -0.36 | -0.36 | 0.33 | -0.02 | 0.02 | -0.56 | -0.35 | 0.50 | -0.56 | **-0.99** | 0.50 | 0.03 | -0.03 |

| Collinearity Conditions with one constraint of Coplanarity Conditions | | Calibration Parameters (CP): First Station | | | | | | | | Second Station | | | | | | | |
|---|---|---|---|---|---|---|---|---|---|---|---|---|---|---|---|---|---|
| | | $ER$ | $EH$ | $EV$ | $a_1$ | $a_2$ | $a_3$ | $a_4$ | $a_5$ | $ER$ | $EH$ | $EV$ | $a_1$ | $a_2$ | $a_3$ | $a_4$ | $a_5$ |
| Exterior Orientation Parameters (EOP) | $\omega$ | **0.71** | -0.69 | **-0.96** | **0.71** | **0.96** | **-0.96** | 0.07 | -0.07 | **0.73** | -0.69 | **-0.97** | **0.73** | 0.50 | **-0.97** | -0.08 | 0.08 |
| | $\varphi$ | -0.61 | 0.58 | **0.86** | -0.61 | **-0.85** | **0.86** | -0.05 | 0.05 | -0.59 | 0.58 | **0.80** | -0.59 | -0.38 | **0.80** | 0.05 | -0.06 |
| | $\kappa$ | **-0.91** | **1.00** | 0.67 | **-0.91** | **-0.73** | 0.67 | -0.03 | 0.03 | **-0.92** | **1.01** | **0.71** | **-0.92** | -0.49 | **0.71** | 0.04 | -0.04 |
| | $X_S$ | **-0.90** | **1.00** | 0.66 | **-0.90** | **-0.72** | 0.66 | -0.03 | 0.03 | **-0.91** | **1.00** | **0.70** | **-0.91** | -0.49 | **0.70** | 0.03 | -0.03 |
| | $Z_S$ | -0.36 | 0.38 | 0.33 | -0.36 | -0.36 | 0.33 | -0.02 | 0.02 | -0.56 | 0.38 | 0.50 | -0.56 | **-0.98** | 0.50 | 0.03 | -0.03 |

Table 3. Precision ($1\sigma$) of selected parameters under the constraint of $X_S$ as the base.

| parameters | Precision | | | | | | | | | | | | | | | |
|---|---|---|---|---|---|---|---|---|---|---|---|---|---|---|---|---|
| | Exterior orientation Parameters (EOP) | | | | | Calibration Parameters (CP) | | | | | | | | Object Points (OP) | | |
| | $\omega$ | $\varphi$ | $\kappa$ | $Y_S$ | $Z_S$ | $ER$ | $EH$ | $EV$ | $a_1$ | $a_2$ | $a_3$ | $a_4$ | $a_5$ | $X$ | $Y$ | $Z$ |
| First station | – | – | – | – | – | 0.2 *mm* | 3″ | 11″ | 0.2 *mm* | 0.6 *mm* or 2′6″ | 11″ | 4″ | 0.2″ | 0.3 *mm* | 0.1 *mm* | 0.2 *mm* |
| Second station | 24″ | 7″ | 1″ | 0.3 *mm* | 1 *mm* | 0.2 *mm* | 3″ | 14″ | 0.2 *mm* | 0.1 *mm* or 6′11″ | 14″ | 4″ | 0.2″ | | | |

Table 4. Correlation matrix between CP of both scan stations and EOP of the second scan station.

| Collinearity Conditions with one constriant of Coplanarity Conditions | | Calibration Parameters (CP) | | | | | | | | | | | | | | | |
|---|---|---|---|---|---|---|---|---|---|---|---|---|---|---|---|---|---|
| | | First Station | | | | | | | | Second Station | | | | | | | |
| | | $ER$ | $EH$ | $EV$ | $a_1$ | $a_2$ | $a_3$ | $a_4$ | $a_5$ | $ER$ | $EH$ | $EV$ | $a_1$ | $a_2$ | $a_3$ | $a_4$ | $a_5$ |
| Exterior Orientation Parameters (EOP) | $\omega$ | **0.71** | 0.20 | **-0.96** | **0.71** | **0.96** | **-0.96** | 0.07 | -0.07 | **0.73** | 0.48 | **-0.97** | **0.73** | 0.49 | **-0.97** | -0.08 | 0.08 |
| | $\varphi$ | -0.60 | -0.19 | **0.86** | -0.60 | **-0.85** | **0.86** | -0.05 | 0.05 | -0.59 | -0.43 | **0.79** | -0.59 | -0.37 | **0.79** | 0.05 | -0.06 |
| | $\kappa$ | -0.21 | -0.09 | 0.44 | -0.21 | -0.42 | 0.44 | -0.09 | 0.09 | -0.25 | 0.22 | 0.43 | -0.25 | -0.23 | 0.43 | 0.28 | -0.29 |
| | $Y_S$ | **-0.90** | -0.68 | 0.66 | **-0.90** | **-0.72** | 0.66 | -0.03 | 0.03 | **-0.91** | **-0.87** | **0.70** | **-0.91** | -0.48 | **0.70** | 0.03 | -0.03 |
| | $Z_S$ | -0.36 | -0.15 | 0.33 | -0.36 | -0.36 | 0.33 | -0.02 | 0.02 | -0.56 | -0.36 | 0.50 | -0.56 | **-0.99** | 0.50 | 0.03 | -0.03 |

The important notion is $\kappa, EH$ and $a_2$ are more precisely estimated compared to both above conditions. It shows there will be a greater number of decorrelated CP that could be independently estimated (Table 4). To the certain extent, the result shows the reasonable comparison with the collinearity conditions.

Adding the constraints in the direction of $X_S$ leads to decorrelated estimation of CP with $\kappa$. It is a very favourable result. The fact confirms that the horizontal plane became more consistent than $Y_S$ constraint.

The existing correlation between rotational parameters $\omega$ and $\varphi$ with the same CP in Tables 3 and 4 indicates the other rotational parameter must be added to reconstruct the coplanarity conditions. Therefore, to resolve the situation, it is recommended that ideally the $\omega$ rotation angle around $X_S$ is simultaneously imposed as the constraints. Tables 5 and 6 show the precision and correlation after imposing these two constraints.

Table 5. Precision $(1\sigma)$ of selected parameters under two constraints of coplanarity conditions in collinearity conditions.

| parameters | Precision | | | | | | | | | | | | | | |
|---|---|---|---|---|---|---|---|---|---|---|---|---|---|---|---|
| | Exterior Orientation Parameters (EOP) | | | | Calibration Parameters (CP) | | | | | | | | Object Points (OP) | | |
| | $\varphi$ | $\kappa$ | $Y_S$ | $Z_S$ | $ER$ | $EH$ | $EV$ | $a_1$ | $a_2$ | $a_3$ | $a_4$ | $a_5$ | $X$ | $Y$ | $Z$ |
| First station | – | – | – | – | 0.1 *mm* | 1" | 3" | 0.1 *mm* | 0.2 *mm* or 35" | 3" | 3" | 0.2" | 0.2 *mm* | 0.1 *mm* | 0.2 *mm* |
| Second station | 3" | 1" | 0.2 *mm* | 0.8 *mm* | 0.1 *mm* | 1" | 3" | 0.1 *mm* | 1 *mm* or 3'16" | 3" | 2" | 0.2" | | | |

Table 6. Correlation matrix between CP and EOP.

| Collinearity Conditions with two constriants of Coplanarity Conditions | | Calibration Parameters (CP) | | | | | | | | | | | | | | | |
|---|---|---|---|---|---|---|---|---|---|---|---|---|---|---|---|---|---|
| | | First Station | | | | | | | | Second Station | | | | | | | |
| | | $ER$ | $EH$ | $EV$ | $a_1$ | $a_2$ | $a_3$ | $a_4$ | $a_5$ | $ER$ | $EH$ | $EV$ | $a_1$ | $a_2$ | $a_3$ | $a_4$ | $a_5$ |
| Exterior Orientation Parameters (EOP) | $\varphi$ | 0.03 | -0.04 | 0.21 | 0.03 | -0.15 | 0.21 | 0.03 | -0.03 | 0.13 | -0.03 | -0.33 | 0.13 | 0.12 | -0.33 | -0.03 | 0.03 |
| | $\kappa$ | 0.51 | 0.33 | -0.06 | 0.51 | 0.25 | -0.06 | 0.01 | -0.01 | 0.50 | **0.91** | -0.18 | 0.50 | 0.21 | -0.18 | 0.18 | -0.18 |
| | $Y_S$ | **-0.81** | **-0.75** | 0.04 | **-0.81** | -0.34 | 0.04 | 0.04 | -0.04 | **-0.83** | **-0.80** | 0.25 | **-0.83** | -0.26 | 0.25 | -0.06 | 0.07 |
| | $Z_S$ | -0.16 | -0.08 | -0.06 | -0.16 | -0.05 | -0.06 | 0.01 | -0.01 | -0.46 | -0.16 | 0.63 | -0.46 | **-0.98** | 0.63 | 0.00 | 0.00 |

Compared to Tables 1 and 3, there is a significant improvement in estimation of the parameters. It is obvious that adding one translation and its rotation results in higher precision and lower correlation of calibration parameters of TLS.

The following outcomes are worthwhile to mention. *Firstly*, the correlation between $\varphi$ and CP in both stations has significantly reduced below the threshold (Tables 2 and 4). *Secondly*, existing correlation in the direction of $Y_S$ - between $Y_S$ and $ER$ and $Y_S$ and $a_1$ - compared to Table 4 was enhanced. *Furthermore*, although $a_2$ is no longer correlated with $Y_S, EH$ correlation shifts from $Y_S$ of the fist scan to $\kappa$ of the second scan station. *Finally*, the transit offset $a_2$ is highly correlated with $Z_S$, and no solutions above can control this issue.

Consequently, it is inferred that the inconsistency in the horizontal plane can be checked as the result of imposing one translation and its rotation. The current situation is able to guarantee the acceptable precision and consistent correlation of the parameters by solving 4 EOP of every scan station with the existence of coplanarity conditions rather than collinearity conditions. The existing correlation between transit offset – offset of horizontal plane with respect to the origin of coordinate system changing the vertical angle and range – and $Z_S$ will not be reduced as the result of those conditions. Table 5 illustrated if the precision of estimation for range and angular parameters is accurate enough (e.g., within $\pm 1\ mm$ or 3", respectively), we might be able to expect reasonable correlation between those parameters. In order to address the issue of precision, it is sufficient to study the first order of geodetic network design (FOD).

## 5. CONCLUSIONS

To summarise, this research aimed to investigate the correlation of calibration parameters associated into self-calibration of TLS. The implementation under two conditions of SFM – collinearity conditions and collinearity conditions with the constraints of coplanarity conditions - without the aid of prior information of object points for datum definition has been completed. It is clearly seen adding one constraint of relative orientation such as base, slope distance between two origins of scanner coordinate systems, to construct the coplanarity conditions, does not necessarily improve the precision and correlation of parameters, although the inner correlation between parameters is still a debateable issue. On the other hand, it was proven that applying two constraints of relative orientation into the BBA of self-calibration alongside rigorous scanning geometry and robust outlier detection are able to enhance the precision and correlation of eight chosen calibration parameters and exterior orientation parameters. The future investigation will be implementation of the principle on the entire 21 calibration parameters of TLS. In addition to that, a greater number of EOP in case of having more scan stations must be solved. Furthermore, the detection of outliers – to check internal and external reliability - prior to implementing the algorithm must not be underestimated. Finally, the recommendation of the simultaneous evaluation of the other orders of the network – first and second order design (FOD) and (SOD) – provides better insight of all criteria of the network.

## REFERENCES

Alsadik, B. & Abdulateef, N. A., 2022. Epipolargeometry between photogrammetry and computer vision - a computation guide. *ISPRS Annals of the Photogrammetry, Remote Sensing and Spatial Information Sciences,* pp. 25-32.

Amiri-Simkooei, A. R., 1998. Analytical Methods in Optimization and design of Geodetic Networks. *Master's thesis (University of Khaje Nasir Toosi (KNTU)).*

Amiri-Simkooei, A. R., Asgari, J., Zanganeh-Nejad, F. & Zaminpardaz, S., 2012. Basic Concepts of Optimization and Design of Geodetic NEtworks. *Journal of Surveying Engineering,* pp. 172-183.

El-Ashmawy, K., 2021. Coplanarity Condition for Photogrammetric Simultaneous and Self-Calibration Block Adjustment. *International Journal of Advances in Scietific Research and Engineering (IJASRE),* pp. 1-14.

El-Ashmawy, K. A., 2015. A comparison study between collinerity condition, coplanarity condition, and direct linear transformation (DLT) method for camera exterior orientation parmeters determination. *Geodesy and Cartography ,* pp. 66-73.

Fraser, C. S., 2001. *Photogrammetric Camera Component Calibration: A Review of Analytical Techniques.* s.l.:s.n.

Grafarend, E. W., 1974. Optimization of Geodetic Network. *The Canadian Survors ,* pp. 716-723.

Gruen, A., a. H. S. T., 2010. *Calibration and Orientation of Cameras in Computer Vision.* s.l.:Springer.

Holst, C., Artz, T. & Kuhlmann, H., 2014. Biased and unbiased estimates based on laser scans of surface with unknown deformations. *Journal of Applied Geodesy,* 8(3), pp. 169-183.

Holst , C., Medic , T. & Kuhlmann, H., 2018. Dealing with systematic laser scanner errors due to misalignement at area-based deformation analyses. *Journal of Applied Geodesy.*

Jafar, H. A., Meng , X. & Sowter, A., 2018. Terrestrial laser scanner error quantification for the purpose of monitoring. *Survey Review,* 50(360), pp. 232-248.

Kresten, T. P. & Lindstaedt , M., 2022. Geometric Accuracy Investigations of Terrestrial Laser Scanner Systems in the Laboratory and in the Field. *Journal of Applied Geomatics,* pp. 421 - 434.

Lichti, D. D., 2007. Error modelling, calibration and analysis of an AM-CW terrestrial laser scanner system. *ISPRS Journal of Photogrammetry and Remote Sensing,* pp. 307-324.

Lichti, D. D., Pexman , K. & Tredoux, W., 2021. New method for first order network design applied to TLS self-calibration networks. *ISPRS Journal of Photogrammetry and Remote Sensing,* pp. 306-318.

Li, X., Li, Y., Xie , X. & Xu, L., 2018. Lab-built terrestrial laser scanner self-calibration using mounting angle error correction. *Optics Express,* 26(11).

Li, X., Xie, X. & Xu, L., 2018. Terrestrial laser scanner autonomous self-calibration with no prior knowledge of point-clouds. *IEEE Sensors ,* 18(22), pp. 9277-9285.

Medic, T., Kuhlmann, H. & Holst , C., 2019. *Automatic in-situ self-calibration of a panoramic TLS from a single station using 2D keypoints.* Eschede, the Netherlands , s.n.

Mikhail, E. M., Bethel , J. S. & McGlone , J. C., 2001. *Introduction to Modern Phtogrammetry.* The USA : John Wiley & Sons .

Muralikrishnan, B., 2021. Performance evaluation of terrestrial laser scanners—a review. *Measurement Science and Technology.*

Muralikrishnan, B. et al., 2015. Volumetric performace evaluation of a laser scanner based on geometric error model. *Precision Engineering,* pp. 139 - 150.

Pareja, T. F., Pablos , A. G. & Oliva, J. D. V. Y., 2013. Terrestrial Laser Scanner (TLS)Equipment Calibration. *Procedia Engineering ,* Volume 63, pp. 278-286.

Reshetyuk, Y., 2009. Self-calibration and direct georeferencing in terrestrial laser scanning. *PhD Thesis, KTH University .*

Reshetyuk, Y., 2010. A unified approach to self-calibration of terrestrial laser scanners. *ISPRS journal of Photogrammetry and Remote Sensing,* pp. 445-456.